Rensselaer

Human Safety

Virtual Surgery

Suvranu De

J. Erik Jonsson ’22 Distinguished Professor of Engineering

Director, Center for Modeling, Simulation and Imaging in Medicine (CeMSIM)

Head, Department of Mechanical, Aerospace and Nuclear Engineering

Rensselaer Polytechnic Institute, Troy, NY

No disclosures

Collaborating Hospitals:

Beth Israel Deaconess Medical Center (MA)
Massachusetts General Hospital (MA)
Cambridge Health Alliance (MA)
Mount Auburn Hospital (MA)
Tufts University (MA)
Yale University Medical School (CT)
University at Buffalo (NY)
Baylor University Medical Center (TX)
University of Texas Southwestern Medical Center (TX)
University of Texas San Antonio (TX)

Academic Collaborators:

Harvard Medical School
University at Buffalo
Wright State University
University of Central Arkansas

Industrial Partners:

Kitware
Simquest
CFDRC
Infocitex
Charles River Analytics

Surgery is a complex task performed in a complex environment

To Err is Human

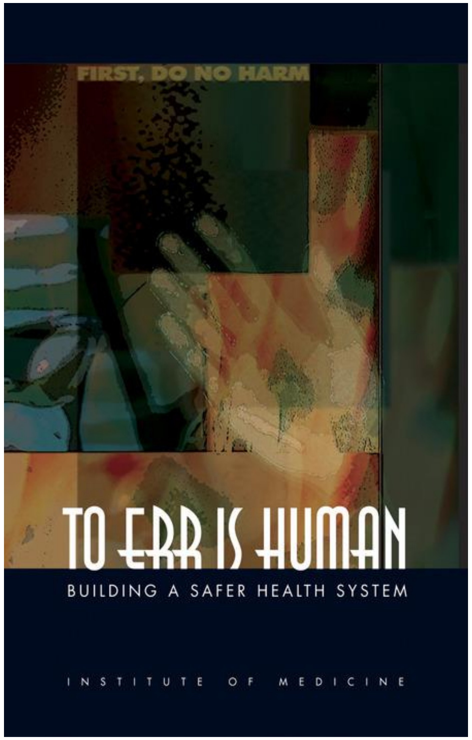

98,000 Americans die per year of medical errors [Institute of Medicine, 1999]

Causes of death in the US, 2013

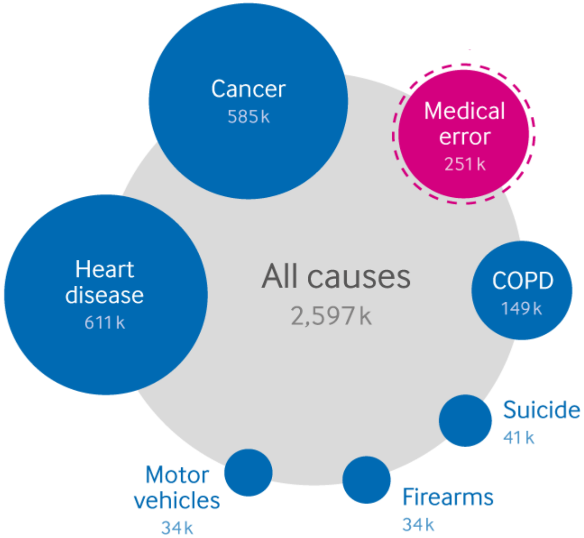

source: http://www.cdc.gov

Residency Model

"The Agnew Clinic" Thomas Eakins, 1889

Challenges of the residency model:

Patient safety

Complex cases

High cost ~ $50K/year/trainee

Subjective assessment

Not adaptive

Primarily procedural skills

Reduced patient contact

- 80 hour work week
- Increased malpractice liability
- Reduced hospital stays

Virtual Intelligent Preceptor

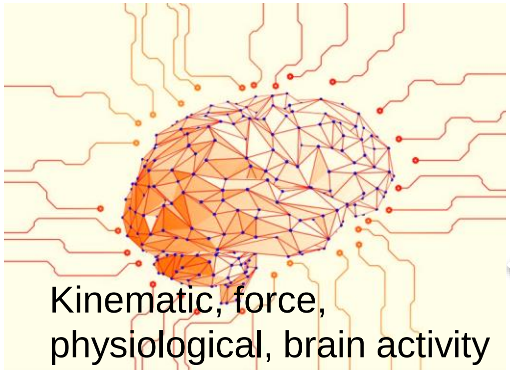

Learner model

Predicts possible actions based on current state

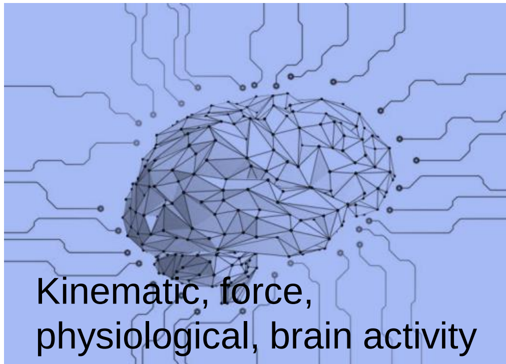

Cognitive model

Predicts possible **correct** actions based on current state

Predicted action

Correct action

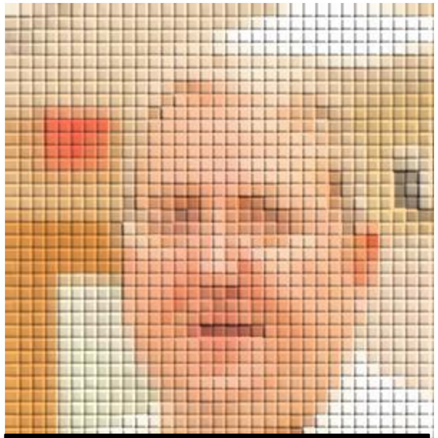

Virtual Preceptor

Selects feedback based on action mismatch

Feedback

Learner

Overall Research

Artificial intelligence

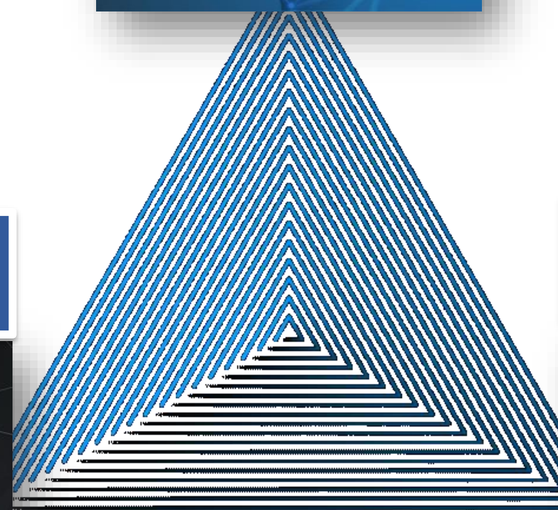

Brain imaging

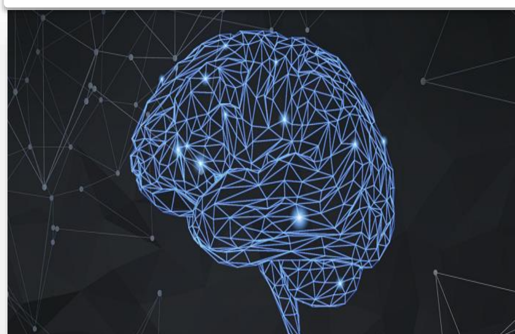

Virtual reality

Enhance Virtual Reality

"True virtual reality creates the illusion of actually being in a difference space. It can be used for training, treatment, and communication"

Technical Challenges

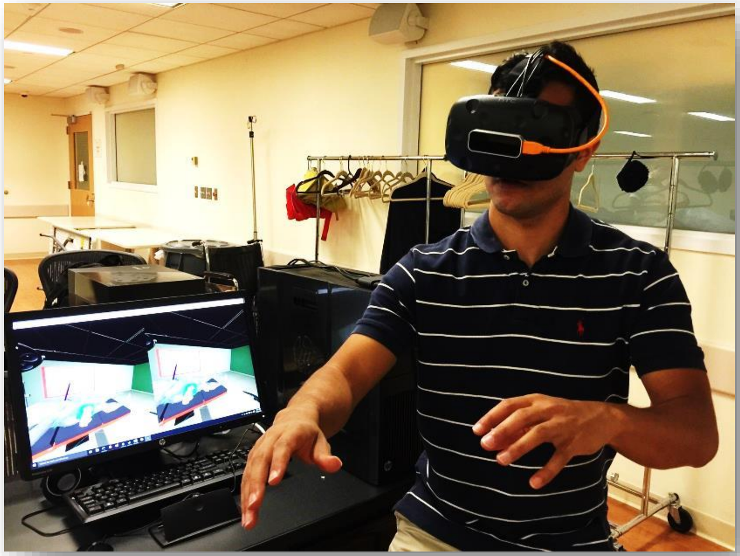

Interactivity

- Real time graphics (min 30 frames/sec)
- Real-time haptics (min 1000 frames/sec)

High fidelity

- Multi-physics
- Multi-phase
- Multi-scale

Electrosurgery

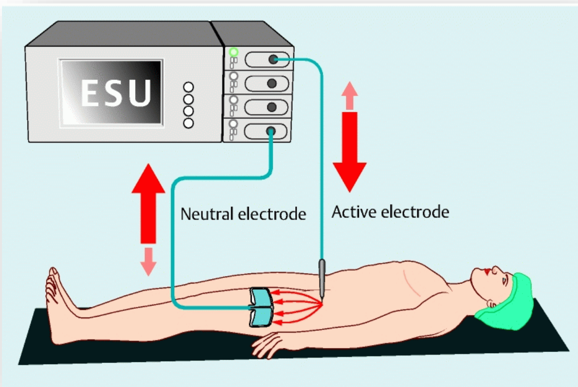

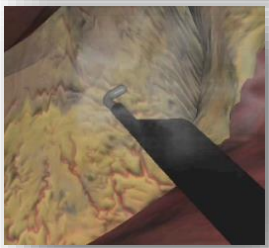

- Widely used to cut and coagulate tissue at the same time.
- 17.5 M procedures annually in the US with 40,000 burn cases
- Heat is generated in the tissue due to radio frequency (0.3-5MHz) electric current.
- With RF current, the large protein ions oscillate in the intra-cellular fluid (cytosol), heating it though kinetic losses

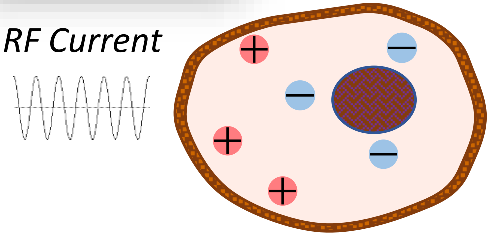

large protein ions
oscillate in the cell
generating heat

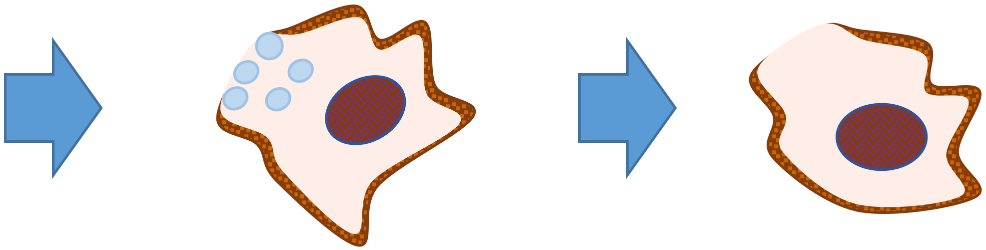

60-100°C
protein denaturization
water evaporation

> 100°C
vaporization of the cell

Electro-surgical Simulations

- Multi-physics (mechanical, thermal, electrical)
- Multi-phase (solid, liquid, vapor)
- Multi-scale (tissue and cellular)

TISSUE LEVEL

Charge conservation:
$\nabla \cdot (\sigma \nabla V) = 0$

$q_f = \mathbf{J} \cdot \mathbf{E}$

Linear momentum balance: $\nabla \cdot \boldsymbol{\sigma} + \mathbf{b} = \mathbf{0}$

$\boldsymbol{\sigma} = -p\mathbf{I} + \boldsymbol{\tau}$

Energy balance:
$\rho \dot{e} = \boldsymbol{\sigma} : \dot{\boldsymbol{\varepsilon}} + q - \nabla \cdot \mathbf{q}$

$q = \rho c \dfrac{\Delta T}{\Delta t}$

CELLULAR LEVEL

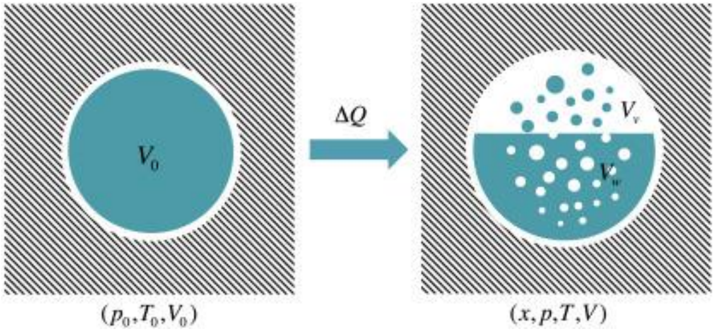

Solve EOS for thermodynamic states (p, T) and effective density, specific heat capacity, thermal conductivity and heat generation.

- Quasi-static Maxwell's $\lambda_{wave} \sim 10^2 m$
- Quasi-static linear momentum

Tissue Dissection

- Level set function

$$\phi(\mathbf{x},t) = \begin{cases} < 0 & \mathbf{x} \in \Omega_h \\ > 0 & \mathbf{x} \in \Omega_d \\ = 0 & \mathbf{x} \in \Gamma_i(t) \end{cases}$$

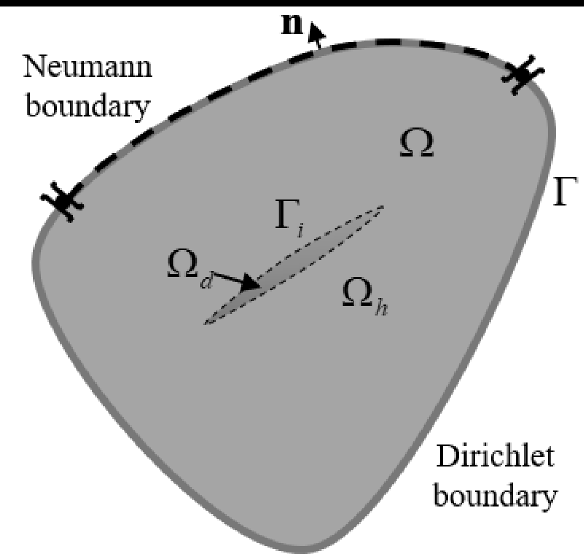

Evolving interface

$\Gamma_i(t) = \{\mathbf{x} | \phi(\mathbf{x},t) = 0\}$.

- Level set evolution equation

$$\frac{\partial \phi}{\partial t} + \mathbf{v} \cdot \nabla\phi = 0$$

Interface velocity

- Free energy functional $\psi = \hat{\psi}(\boldsymbol{\varepsilon}, T, \phi)$
- **Clausius-Duhem** inequality: $\rho\dot{\psi} + \rho\eta\dot{T} - \boldsymbol{\sigma}:\dot{\boldsymbol{\varepsilon}} \leq 0$
- Constitutive relations:
  - Cauchy stress $\boldsymbol{\sigma} = \rho\frac{\partial\psi}{\partial\boldsymbol{\varepsilon}}$
  - Specific entropy $\eta = -\frac{\partial\psi}{\partial T}$
  - Dissipation inequality $\rho\frac{\partial\psi}{\partial\phi}\dot{\phi} \leq 0$

$$\boldsymbol{\sigma} = -p\mathbf{I} + \boldsymbol{\tau}$$

Hydrostatic pressure

Deviatoric stress $\boldsymbol{\tau} = \boldsymbol{\sigma} - \frac{1}{3}tr(\boldsymbol{\sigma})\mathbf{I}$

$$\beta\dot{\phi} = -\rho\frac{\partial\psi}{\partial\phi}$$

$\beta > 0$, Kinetic coefficient

Han, Z., Rahul, De, S. (2018) Comput. Methods Appl. Mech. Eng. 337, 527

Osher, S., & Sethian, J.A. (1988). J Comp Physics, 79, 12-49.

Solution Approach

- Finite element discretization

  Electric potential: $V(\mathbf{x}) = \sum_I N_I(\mathbf{x}) V_I$

  Temperature: $T(\mathbf{x}, t) = \sum_I N_I(\mathbf{x}) T_I(t)$

  Displacement: $\mathbf{u}(\mathbf{x}) = \sum_I N_I(\mathbf{x}) \mathbf{u}_I$

- Linear algebraic equations: $\mathbf{F}^t \equiv \begin{Bmatrix} \mathbf{F}_V \\ \bar{\mathbf{F}}_T \\ \mathbf{F}_u \end{Bmatrix} = \begin{bmatrix} \mathbf{K}_V & \mathbf{0} & \mathbf{0} \\ \mathbf{0} & \bar{\mathbf{K}}_T & \mathbf{0} \\ \mathbf{0} & \mathbf{0} & \mathbf{K}_u \end{bmatrix} \begin{Bmatrix} \mathbf{V} \\ \mathbf{T} \\ \mathbf{U} \end{Bmatrix} \equiv \mathbf{K}^t \mathbf{X}^t$

Solved using Krylov subspace iterative solver (*e.g.* GMRES)

$$\bar{\mathbf{F}}_T = \left(\mathbf{M}_T - \frac{1}{2}\Delta t \mathbf{K}_T\right)\mathbf{T}^t + \Delta t \mathbf{F}_T^{t+\frac{1}{2}\Delta t} \quad \text{(Midpoint rule)}$$

$$\bar{\mathbf{K}}_T = \left(\mathbf{M}_T + \frac{1}{2}\Delta t \mathbf{K}_T\right)$$

Han, Z., Rahul, De, S. (2018) *Comput. Methods Appl. Mech. Eng.* 337, 527.

- Numerical approximation of the level set equation:

$$\phi_I^{t+\Delta t} = \phi_I^t + \Delta t \frac{\sum_l^n \alpha_I^l \int_{T_l} (\psi_e - \kappa)|\nabla \phi| d\Omega}{\sum_l^n \alpha_I^l meas(T_l)}$$

Volume of simplex T_l

Bounded, positive weighting coefficients computed on simplex T_l

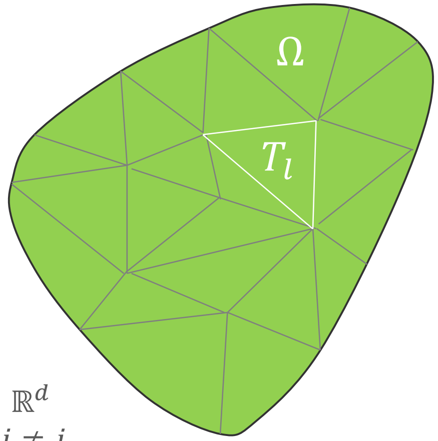

$\mathcal{T}$:= triangulation set in $\mathbb{R}^d$

$\mathcal{T} = \cup T_j$, $T_i \cap T_j = \emptyset$ for $i \neq j$

Hybrid CNN Approach

- **End-to-end learning** – general way of applying deep learning (DL) to simulate a physical system
  - Accumulated errors over the time steps
  - Data inefficiency due to unaccounted interactions between physics
  - Slower to converge
- **Hybrid approach**
  - Use DL to learn computationally expensive component (i.e. solution of linear momentum balance)
  - Use efficient FEM solver to handle interactivity
  - CNN's sparse interaction characteristic enables fewer weight parameters to be trained

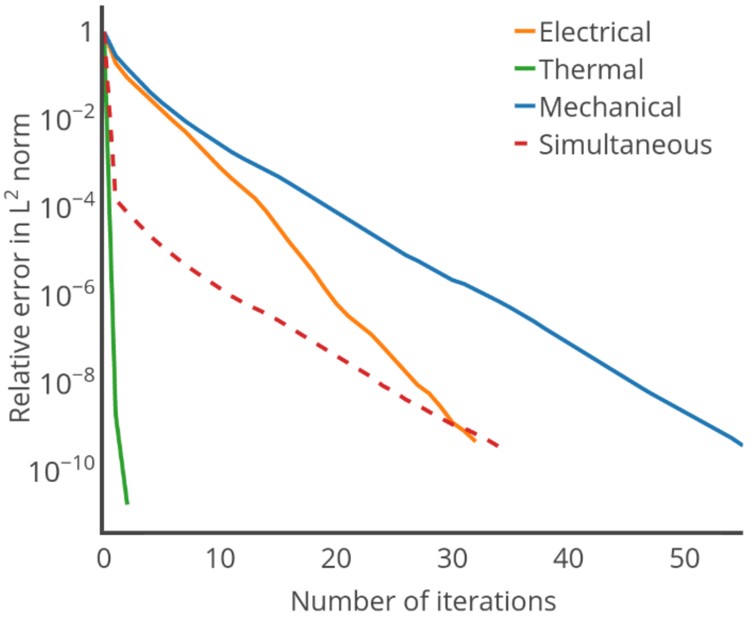

Hybrid CNN Approach

Training

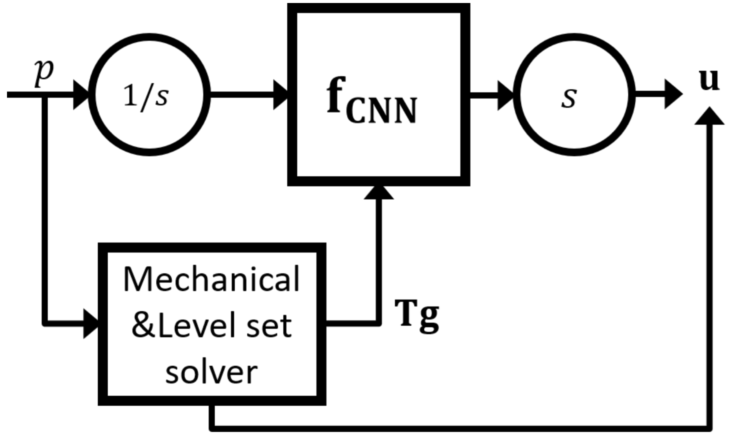

Prediction

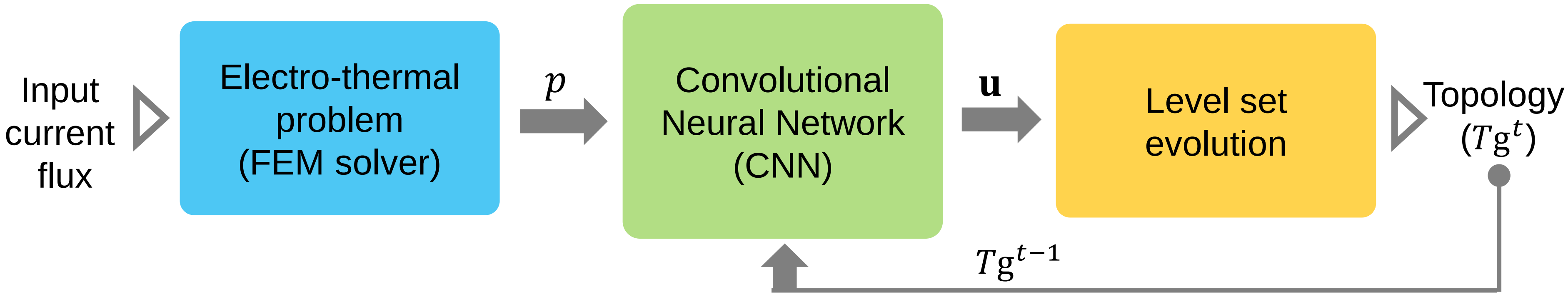

Experimental Validation

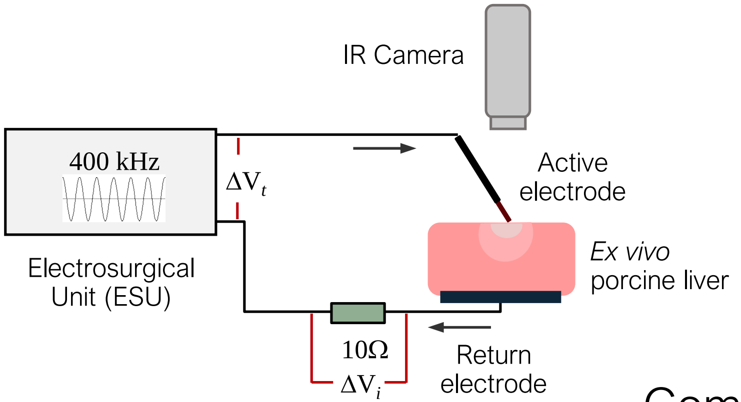

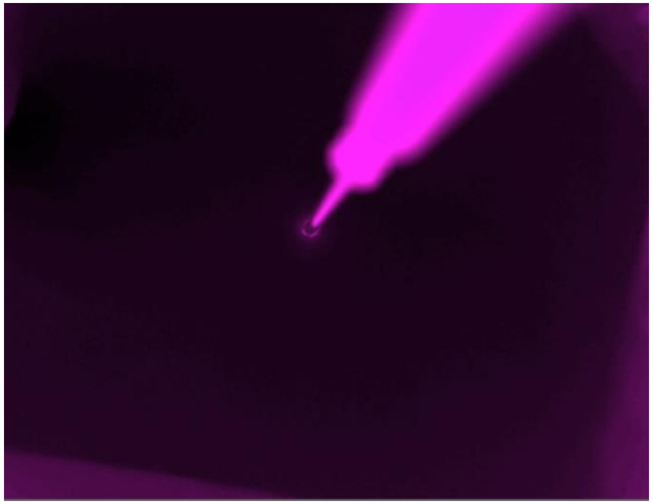

Temperature (℃)

10 80

Karaki *et al.* (2017)
IEEE Trans. Biomed. Eng., 64, 1211.

Comparison of temperature evolution (FEM solver) with the experimental data for *ex vivo* porcine liver

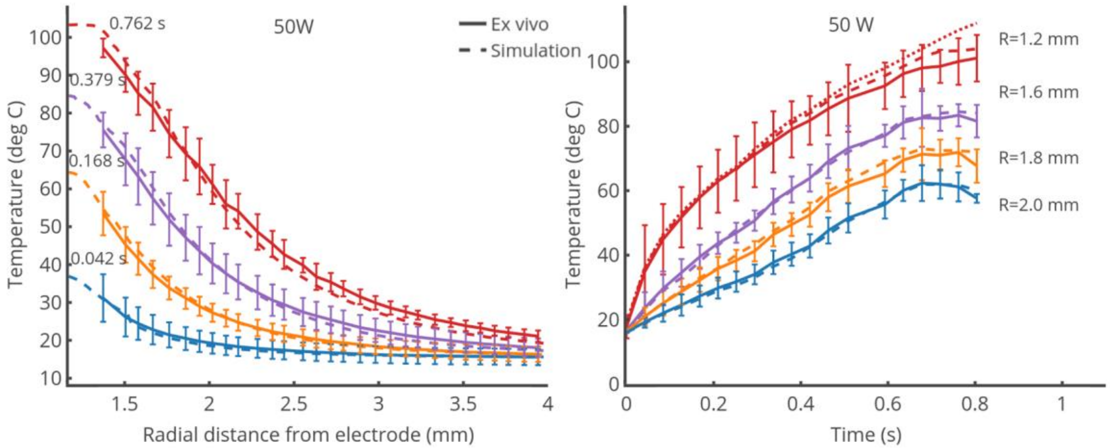

Han, Z., Rahul, De, S. (2018)
Comput. Methods Appl. Mech. Eng. 337, 527.

Static Electrode

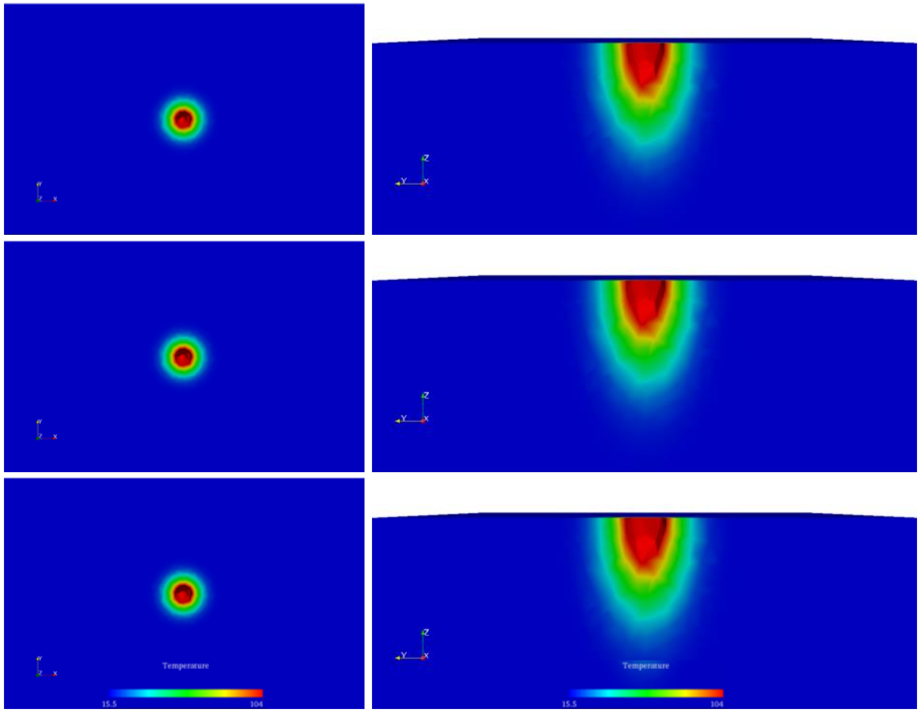

High-fidelity multiphysics model

Hybrid-CNN (L^2 error: 6.9%)

PGD (L^2 error: 13%)

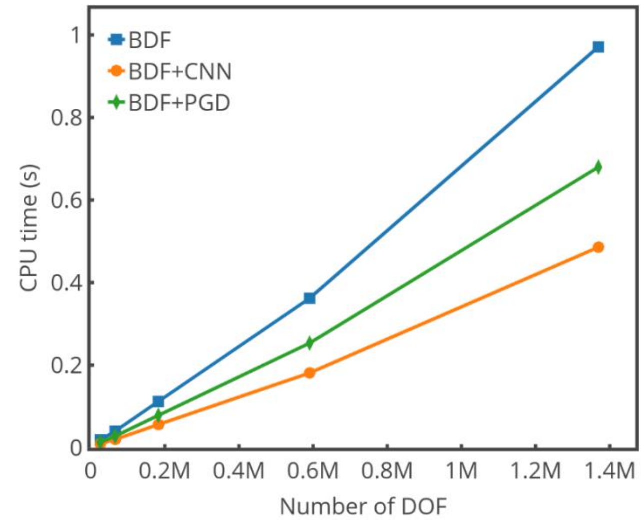

Moving Electrode

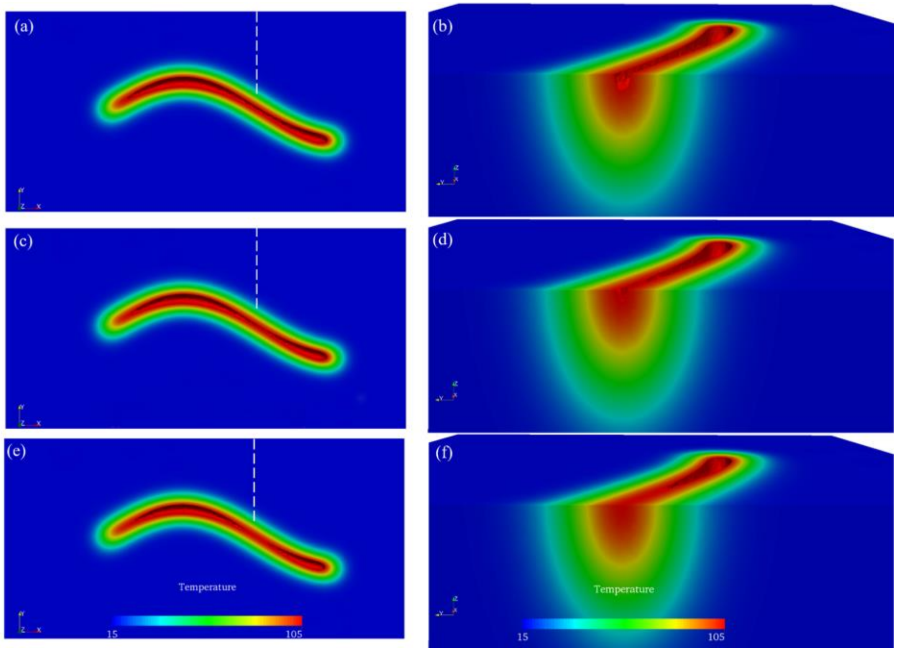

High-fidelity multiphysics model

Hybrid-CNN (L^2 error: 9.6%)

PGD (L^2 error: 30.7%)

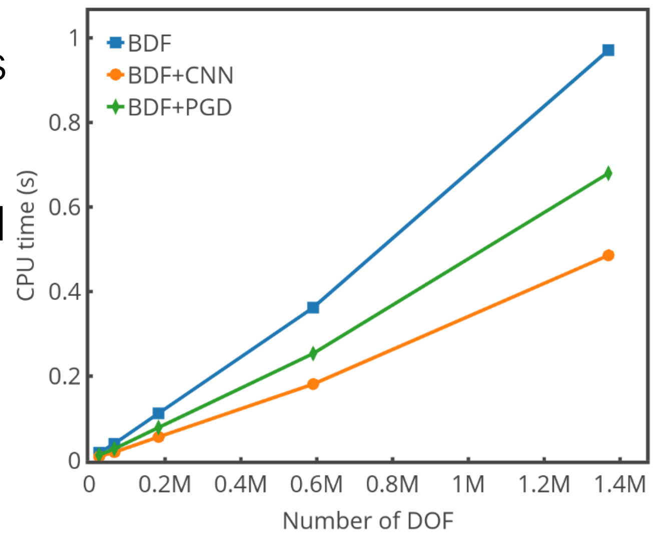

Thank you!

Rensselaer

why not change the world?®